Engineering Structures 204 (2020) 109900

Contents lists available at ScienceDirect

Engineering Structures

journal homepage: www.elsevier.com/locate/engstruct

Shear strength estimation of masonry walls using a panel model

Leonardo M. Massone[a,*], Daslav F. Ostoic[b]

[a] Department of Civil Engineering, University of Chile, Blanco Encalada 2002, Santiago, Chile
[b] University of Chile, Chile

ARTICLE INFO

Keywords:
Shear strength
Panel response
Masonry
Wall
Model

ABSTRACT

Masonry walls are structural elements generally used in housing or small buildings. Given their structural configuration, they commonly present shear failure due to seismic actions, characterized by a fragile response. Thus, it is important to have simple, yet reliable tools that correctly estimate the shear capacity of walls. For that, a simple existing model developed for reinforced concrete elements and based on a panel model is used and adapted to masonry walls, providing a novel formulation that can be applicable to both materials. For compression and tension behavior, the prismatic resistance of the panel is used, which, due to the anisotropy of the material, degrades with the angle formed by the load with the vertical mortar joint. Strain values are set for compression and tension failure modes, and a degradation coefficient in compression due to the biaxial strain loading is included. Additionally, bond failure is also incorporated into the model. A database of 41 tests of reinforced masonry walls and 12 tests of confined masonry walls is used for model validation. The strength ratio between the shear strength obtained by the model and the test is compared, giving an average and a coefficient of variation (COV) of 1.0 and 0.15, respectively for reinforced walls, and 1.08 and 0.14 for confined walls, showing a satisfactory performance and better behavior than simple models from the literature. The analysis of general trends of the strength ratio reveals that there is a low dependence between the strength ratio and the studied parameters, implying that the model captures the physical behavior of masonry walls.

1. Introduction

Masonry is a material used among others in walls for multi-family housing from 1 to 4 stories high or for private single-family houses. In Chile and many other places, these are basically built in two ways: reinforced with vertical and horizontal reinforcing bars in the panel, or confined by a reinforced concrete frame, similar to infill walls, but in this case the frame is built after the masonry wall, such that the masonry panel and the frame are better connected. Masonry is a material characterized by its anisotropy, which affects properties such as compression and tension strengths that change with the loading angle, yielding a complex shear strength mechanism. Seismic behavior of masonry walls, commonly with low aspect ratio, is usually controlled by shear strength and having reliable and yet simple analytical tools to quantify the shear strength and failure mode of masonry walls is required in design.

A panel-type model used to estimate the shear capacity of reinforced concrete walls is described and herein adapted to masonry walls, providing a novel formulation that can be applicable to both materials. The model was originally developed by Kaseem and Elsheikh [1], as an iterative panel model for short reinforced concrete walls. This isolated element is subject to a lateral and axial force and has reinforcement in the longitudinal (L) and transverse (t) directions, which coincide with the vertical and horizontal directions of the wall, respectively (Fig. 1). The base panel model uses average stress and average strain states for the wall panel, imposing equilibrium, strain compatibility and constitutive material laws that govern concrete and reinforcing steel behavior. The concrete material model considers a biaxial behavior, where the principal tensile axial strain, perpendicular to the principal compression direction (forming an angle α with the longitudinal direction), causes a degradation of the compressive response. The vertical and horizontal reinforcement bars contribute to strength in their longitudinal direction, without a dowel action. Two coordinate systems are generated, one given by the reinforcement layout (system "L-t") and another by the concrete principal directions (called system "d-r"), as shown in Fig. 1.

Equilibrium is imposed in the L-t coordinate system determining the concrete stresses in the principal directions (d-r) based on the concrete strains in such directions and the steel stresses in the L-t coordinate. Considering that principal concrete stresses coincide with principal strains, the principal concrete stresses acting in an angle α are σ_d and σ_r. Eqs. (1) and (2) show the longitudinal and shear equilibrium:

* Corresponding author.
E-mail addresses: lmassone@ing.uchile.cl (L.M. Massone), daslav.ostoic@idiem.cl (D.F. Ostoic).

https://doi.org/10.1016/j.engstruct.2019.109900
Received 4 July 2019; Received in revised form 17 September 2019; Accepted 5 November 2019
Available online 28 November 2019

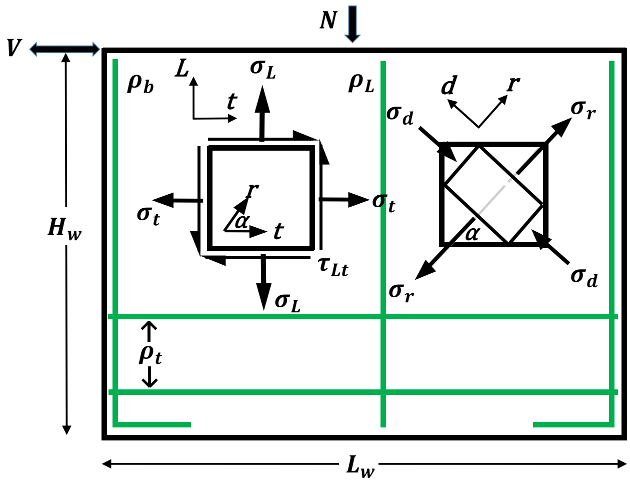

Fig. 1. Masonry wall with stress resultants in L–t coordinates, and in principal direction d – r coordinates.

$$\sigma_L = \sigma_d \cos^2\alpha + \sigma_r \sin^2\alpha + \rho_L f_L \quad (1)$$

$$\tau_{Lt} = (-\sigma_d + \sigma_r)\cos\alpha\sin\alpha \quad (2)$$

where σ_d and σ_r are the axial concrete stress in the d and r directions, σ_L is the longitudinal panel equilibrium stress, τ_{Lt} is the shear stress resultant in the "L-t" system, $\rho_L f_L$ is the steel force per concrete area (steel ratio times stress) in the L direction.

The shear resultant force (V) is expressed as:

$$V = \tau_{Lt} t_w d_w \quad (3)$$

where t_w is the wall thickness and d_w is the length of the wall between the centroids of the boundary elements ($0.8L_w$, if no boundary element exists, with L_w being the wall length).

Strain compatibility in the L-t system is established as,

$$\varepsilon_L = \varepsilon_d \cos^2\alpha + \varepsilon_r \sin^2\alpha \quad (4)$$

$$\varepsilon_t = \varepsilon_d \sin^2\alpha + \varepsilon_r \cos^2\alpha \quad (5)$$

$$\gamma_{Lt} = 2(-\varepsilon_d + \varepsilon_r)\cos\alpha\sin\alpha \quad (6)$$

where ε_L and ε_t are the normal strain in the L and t directions, respectively; γ_{Lt} is the shear strain in the direction L-t; and ε_d and ε_r are the normal principal strain in the directions d and r, respectively. For walls controlled by shear deformations, the lateral wall displacement can be estimated as $\Delta = \gamma_{Lt} H_w$, where H_w is the wall height.

Once the strains are known, a rotating-angle material model is used to evaluate the concrete stresses in the principal directions [2]. The rotating-angle approach is a material model formulation for panel elements (plane stresses) that treats the concrete component as an orthotropic material that is characterized by estimating concrete stresses in two principal directions provided by uniaxial material constitutive laws evaluated with the strains in the correspondent two principal directions (which might rotate). For a simple model, uniaxial compression behavior for concrete follows a parabolic stress-strain relationship that includes a degradation caused by the tensile strains in the orthogonal direction. For tension, the stress-strain relationship is linear until cracking and then degrades linearly to zero. For the reinforcement, perfect bonding to the concrete is assumed and an elastic perfectly-plastic constitutive material law is considered for both the L and t directions.

2. Modifications to the original model

Massone and Álvarez [3] incorporated the effect of the wall boundary reinforcement in the longitudinal equilibrium equation (Eq. (1)), through a parameter β, which represents the contribution of the boundary reinforcement to shear strength. The optimum value of β was 0.3. The equilibrium in the longitudinal direction L is modified as,

$$\sigma_L = \sigma_d \cos^2\alpha + \sigma_r \sin^2\alpha + \rho_L f_L + \beta\rho_b f_b \quad (7)$$

where $\rho_b f_b$ is the boundary longitudinal force per concrete area (steel ratio times the stress).

Massone and Orrego [4] re-calibrated the principal strain angle (α), established by Massone and Ulloa [5], developing a unique expression for walls, deep beams and corbels and another expression for beam-column connections based on strain estimations from finite element analysis [6]. In Eq. (8), the expression for the principal strain angle for simple curvature is shown. Eq. (8) is also applicable to masonry walls experiencing single curvature, i.e., cantilever walls subjected to lateral load at the top of the wall.

$$\alpha = 13.87\left(\frac{H_w}{L_w} + 0.5\right)^{-0.13}\left(\frac{N}{f_c' t_w L_w} + 0.1\right)^{-0.67} \quad (8)$$

Massone and Melo [7] incorporated the transverse reinforcement component to the nominal tensile capacity of the concrete as it was done by Wang et al. [8]. The component associated with the longitudinal reinforcement is not added because its contribution is already incorporated in the longitudinal equilibrium of the panel element (Eqs. (1) and (7)). The final expression for the nominal tensile capacity of the element with these modifications is shown in Eq. (9).

$$f_{ct}' = f_{cto}' + \rho_t f_t \cos^2\alpha \quad (9)$$

where f_{cto}' is the basic tensile strength of concrete and $\rho_t f_t$ is the horizontal web force per concrete area (steel ratio times the stress); the horizontal reinforcement is assumed to have yielded.

The model, including its modifications, using equilibrium, compatibility and non-linear material constitutive laws, allows determining the wall response (force versus displacement) using numerical methods to solve the non-linear equation of longitudinal equilibrium (Eq. (1), later replaced by Eq. (7)). In order to simplify the methodology, Massone and Melo [7] instead of performing an incremental analysis to obtain the complete wall response (shear force-displacement curve) focused on calculating shear strength values for each type of potential failure in the model by setting the material strain at the material capacity, which for reinforced concrete elements corresponds to: (i) concrete in compression (ε_d associated with σ_d), (ii) concrete in tension (ε_r associated with σ_r), and (iii) yielding of web and boundary reinforcement (ε_L associated with f_L and f_b since it uses the same strain), whose terms appear in Eq. (7). The solution of the nonlinear Eq. (7) is replaced by calibrated expressions of strain (ε_d* for tension failure of concrete or reinforcement yielding, and ε_r* for compression failure of concrete) that closely reproduces the results of such an equation [7]. Thus, given a failure mode, a strain value is fixed (ε_d for (i), ε_r for (ii) or ε_L for (iii)), which together with a calibrated strain expression (ε_d* for (ii) and (iii) or ε_r* for (i)) and the known principal strain/stress direction angle (α), the strain field is identified allowing determining the stress values in both materials and therefore the shear strength (V). A calibration was performed for ε_d* and ε_r* in order to better reproduce the results obtained with the iterative model that solves the nonlinear Eq. (7). The expressions for the different failure modes, i.e., tension (Eq. (10)), compression (Eq. (11)), and reinforcement yielding (Eq. (12)), are shown in Eqs. (10)–(12).

$$\varepsilon_d^* = -1.292x10^{-3}(cos\alpha)^{-2.56}\left(\frac{N}{f_c' A_g} + 0.1\right)^{1.40} \quad (10)$$

$$\varepsilon_r^* = 3.610x10^{-4}\left(\frac{\rho_L f_{yL}}{f_c^{'}} + 0.05\right)^{-0.59}\left(\frac{\beta\rho_b f_{yb}}{f_c^{'}} + 0.05\right)^{-0.60}(\cos\alpha)^{3.46}\left(\frac{N}{f_c^{'}A_g} + 0.1\right)^{-0.86} \quad (11)$$

$$\varepsilon_d^* = -0.635\left(\frac{\rho_L f_{yL}}{f_c^{'}} + 0.05\right)^{1.24}\left(\frac{\beta\rho_b f_{yb}}{f_c^{'}} + 0.05\right)^{1.22}(\cos\alpha)^{-2.45}\left(\frac{N}{f_c^{'}A_g} + 0.1\right)^{1.36} \quad (12)$$

where $N/f_c^{'}A_g$ is the axial stress normalized by the concrete compressive strength ($f_c^{'}$), and f_{yb} and f_{yL} are the boundary and longitudinal web yield stress, respectively.

Once strength values for all failure models are determined, it is necessary to check if they can be reached. If the shear strain required to reach the compressive strength of the concrete occurs before the shear strain required for yielding of the longitudinal web or boundary reinforcement is reached, then the failure mode is associated with concrete failure. Conversely, if yielding of the reinforcement is reached at an earlier shear strain than that for the concrete compression failure, then the failure mode is associated with reinforcement yielding.

3. Adaptation to masonry walls

The present work aims to adapt this closed-form model developed for reinforced concrete elements to masonry walls, for both reinforced and confined masonry walls. Moreover, the model for strength estimation is validated against a database of masonry wall.

Reinforced masonry walls are composed by a masonry panel with vertical reinforcement installed and grouted in the holes of the masonry units and horizontal reinforcement embedded in grout between lines of masonry units (Fig. 2a), while confined masonry walls are constructed with the masonry panel and a reinforced concrete frame surrounding the panel (Fig. 2b). Considering that the masonry panel can be assimilated to a concrete panel and the reinforcement is present in masonry and reinforced concrete solutions, some failure modes can be also assimilated. Masonry walls have different failure mechanisms when subjected to a lateral load, but there are four main mechanisms related to shear strength: (i) diagonal tension, (ii) diagonal compression, (iii) yielding of reinforcement and (iv) bond, which corresponds to cracking either in the mortar joints, in a row of masonry units or with a staggered pattern. Also, flexural failure can occur.

The following sections define the modifications required to adapt such failure modes in the model according to the material characteristics. Tensile and compression failure are considered similar as that of a reinforced concrete wall, such that, shear failure due to diagonal tension and diagonal compression failure are similar in reinforced concrete and masonry, provided that adherence of masonry joint is strong. Besides, an additional model is included to capture bond failure. The constitutive material laws for masonry in compression and tension, analogous to the case of concrete, are shown in Fig. 3a and b, respectively; whereas steel is shown in Fig. 3c.

3.1. Reinforcing steel

Similar to other formulations, in the case of steel, a uniaxial elastic perfectly-plastic constitutive material law (Fig. 3c) is implemented for all reinforcing steel. Thus, when yielding is reached $\varepsilon_L = \varepsilon_y$ and consistently $f_L = f_b = f_y$.

3.2. Masonry under compression

A difference with reinforced concrete in compression is that the compressive strength of masonry is determined by testing a prism, consisting of a series of units stacked on top of each other and joined with mortar. The prismatic resistance (f'_m) is obtained under compression testing. However, such value does not account for slenderness effect or anisotropy of the material.

Page and Marshall [9] conducted a series of uniaxial compression tests on prisms with different aspect ratios (ratio between the height and width of the unit) to evaluate the influence of this parameter on the prismatic strength. For low aspect ratios, the compressive strength requires a correction due to artificial strength increase caused by constrain at element ends that affects the overall element behavior. A common prism slenderness of 4 is used in tests (including the database used in this work), resulting in a compression strength correction of $K_c = 0.93$.

Masonry is an anisotropic material, such that there is a variation of uniaxial compression strength of the element with the direction of the axial load relative to the unit orientation. Hamid and Drysdale [10] tested 17 specimens, without grouted holes, at different angles α, between the applied compression direction and the vertical prism joint (Fig. 4a). Three prisms were tested for each angle orientation of α = 15°, 45°, 60°, 75° and 90°, and 6 prisms for α = 0°. The strength reduction factor is then defined as the ratio between the strength at a specific orientation (α) and the strength at α = 0°, as $C_\alpha = f'm(\alpha)/f'm(0^\circ)$ (Fig. 4b).

The coefficient C_α is calibrated as,

$$C_\alpha = 2.26\cdot10^{-7}\alpha^4 - 3.42\cdot10^{-5}\alpha^3 + 1.48\cdot10^{-3}\alpha^2 - 0.022\alpha + 1 \quad (13)$$

The panel model requires the strain value associated with the maximum compression stress in the element. Naraine and Sinha [11], for biaxial compression, suggest $\varepsilon_0 = 0.0035$ for ceramic bricks, and Hidalgo [12] a value of $\varepsilon_0 = 0.003$ for concrete blocks. Considering that the compressive strength is reached, the compressive strain at peak strength is $\varepsilon_d = -\xi\varepsilon_o$ and the strength is $\sigma_d = -\xi f_m^{'}$ (Fig. 3a), where ξ represents a strength and strain softening coefficient (reduction) in the compressive direction due to tensile strains in the opposite direction

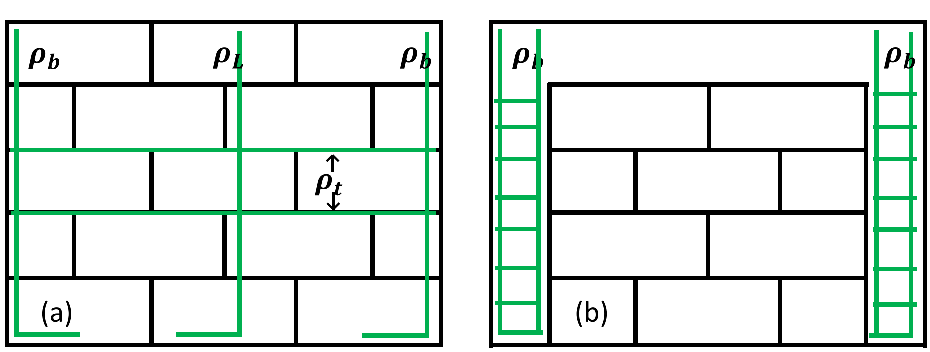

Fig. 2. (a) reinforce masonry wall, and (b) confined masonry wall.

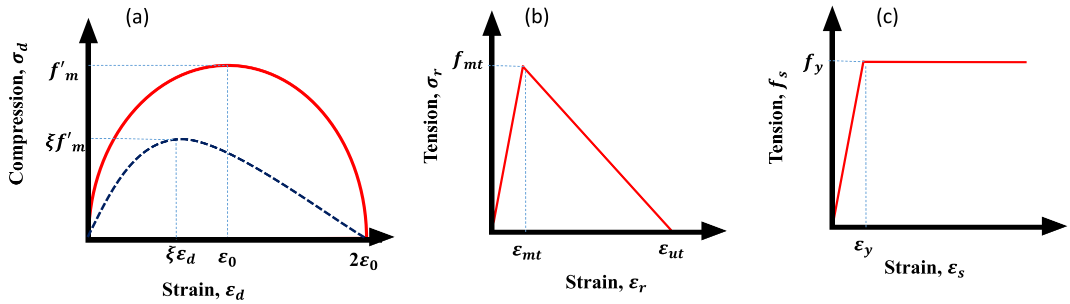

Fig. 3. Material constitutive laws – (a) masonry in compression, (b) in tension, and (c) steel.

(ε_r). Considering a ξ factor consistent with the concrete behavior, the expression is defined as [13],

$$\xi = \frac{5.8}{\sqrt{f'm}} \cdot \frac{1}{\sqrt{1+\gamma\varepsilon_r}} \leq \frac{0.9}{\sqrt{1+\gamma\varepsilon_r}} \tag{14}$$

where γ is a parameter that depends on the type of material subjected under biaxial stress state (400 for reinforced concrete [13]). For this work, a value equal to 2500 is used for all specimens, which yields the best results for the model. For simplicity, a large and refined set of values of γ was implemented, selecting the optimum value.

3.3. Masonry under tension

Tomazevic [14], states that the tensile strength of masonry, f'_{mt}, can be calculated as 3% of the prismatic resistance (f'_m), for units with similar strength to those used in this work. Similar to compression, Drysdale and Hamid [15] tested axial tensile prisms to evaluate the variation of stress for different loading direction angles. Three tests for each inclination angle were performed for α = 45° and 90°, and four specimens for α = 0°. Thus, the tension reduction factor $C_{t\alpha} = \mathrm{f'm}(\alpha)/\mathrm{f'm}(90^{\circ})$, is calculated based on the average data reported by Drysdale and Hamid [15] as shown in Fig. 4c.

$$C_{t\alpha} = 1.47 \cdot 10^{-4}\alpha^2 - 0.0058\alpha + 0.33 \tag{15}$$

The tensile strain at peak tensile strength is generally low [16], which is estimated as $\varepsilon_{mt} = 0.0001$ parallel to the horizontal joint as suggested by Drysdale and Hamid [15]. After reaching the peak strength, the tensile response is assumed to reduce linearly until a zero-stress value for a strain of $\varepsilon_{ut} = 0.00035$ (Fig. 3b).

3.4. Masonry bond

Bond failure occurs when there is a stepped cracking pattern through the joints in the masonry panel due to mortar-unit failure. Dialer [17] proposed a bond model for masonry panels, which applies a Mohr-Coulomb strength model for elements prone to bond failure between the unit and mortar. Units of height b and length d are subjected to normal (f_n and f_p) and shear stresses (τ_{xy} and τ_{yx}), which are part of panel elements under global uniaxial normal principal stresses f_1 and f_2 as shown in Fig. 5a. According to Dialer [17], the normal stresses acting on the unit can be related by a factor χ, as $\chi = \frac{f_n}{f_p}$.

According to Charry [18], there is a moment decompensation that must be balanced by the addition and subtraction of a normal stress Δf_n that tend to cause lifting of half part of the unit (reduced normal stress). The work by Crisafulli [19], for an elastic model of the masonry panel derives an estimation of the additional stress as $\Delta f_n = \frac{1.5 \cdot b \cdot (\tau_{yx} - \tau_{xy})}{d}$. Based on a Mohr-Coulomb strength criterion and considering a unit basic material shear strength as τ_{0xy} and τ_{0yx} (shear strength for zero normal stress), and coefficients of friction between the unit and the mortar as μ_{xy} and μ_{yx}, the bond shear model is defined as $\tau_{yx} = \tau_{0yx} + \mu_{yx} \cdot f_n$ and $\tau_{xy} = \tau_{0xy} + \mu_{xy} \cdot \chi \cdot f_n$. According to Dialer [17], there is a quality factor, F, given the difference between the properties of the horizontal and vertical joints, which is represented by $F = \frac{\tau_{0xy}}{\tau_{0yx}} = \frac{\mu_{xy}}{\mu_{yx}}$. According to the stress state presented in Fig. 5b, a bond failure occurs when f_n is reduced by the effect of Δf_n, that is, when the unit vertical normal stress is $f_n - \Delta f_n$. Then, reorganizing the expressions, it yields

$$\tau_{yx} = \tau^* + \mu^* \cdot f_n \tag{16}$$

where $\tau^* = \frac{\tau_{0yx} \cdot (1 + \mu_{yx} \cdot 1.5 \cdot \frac{b}{d} \cdot F)}{1 + \mu_{yx} \cdot 1.5 \cdot \frac{b}{d}}$ and $\mu^* = \frac{\mu_{yx} \cdot (1 + \mu_{yx} \cdot 1.5 \cdot \frac{b}{d} \cdot \chi \cdot F)}{1 + \mu_{yx} \cdot 1.5 \cdot \frac{b}{d}}$.

Assuming that the compression is larger than tension (f_1 larger than f_2), then $\tau = f_1 \cdot cos(\theta) \cdot sin(\theta) = \tau^* + \mu^* \cdot f_1 sin^2(\theta)$, where θ is the complement of α ($\theta = \pi/2 - \alpha$), which yields,

$$\tau = \frac{\tau^*}{(1 - \mu^* \cdot tan(\theta))} \tag{17}$$

According to a review of tests on mechanical properties of masonry,

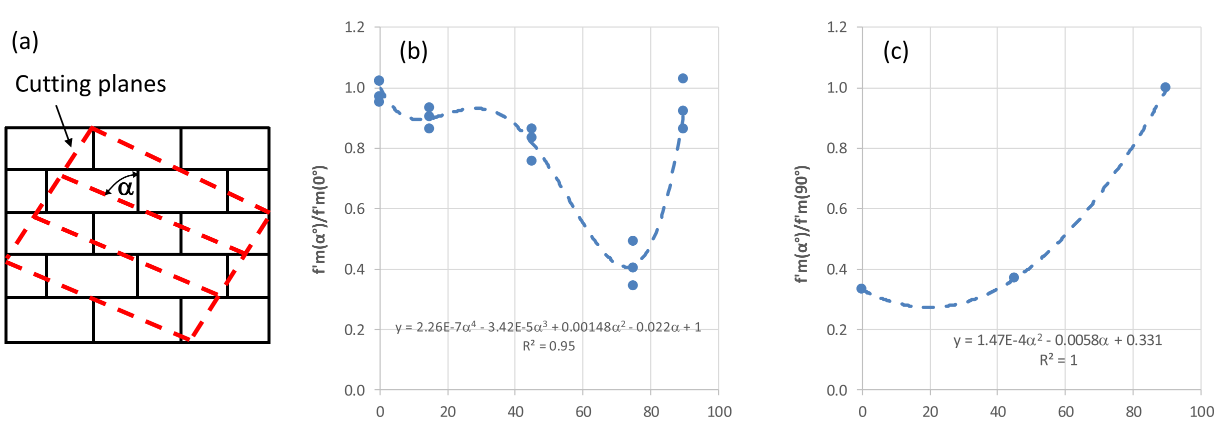

Fig. 4. Prism under uniaxial loading in different directions – (a) prism cutting, (b) under compression, and (c) under tension.

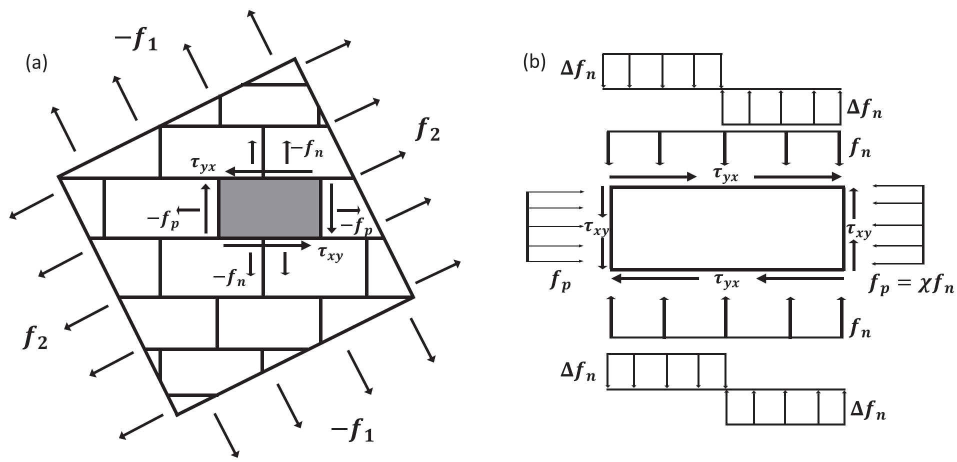

Fig. 5. Bond model – (a) prism under principal stress state, and (b) unit stress state (after [17]).

Cabezas [20] determined that the values of coefficient of friction are μ = 0.7 for ceramic bricks, and μ = 0.8 for concrete blocks. The determination of the basic adhesion strength is carried out by triplet tests. Out of the triplet tests carried out by Fernández [21], there is a series of test elements that represent the mortar used in the wall masonry of the database, yielding a basic adhesion strength of $\tau_0 = 0.56$ MPa. According to Delfín and Bullemore [22], for walls built with concrete blocks and with a mortar paste similar to the walls of the database used in this article, the value of the basic resistance to adhesion corresponds to $\tau_0 = 0.38$ MPa.

The quality factor F relates the basic adhesion and the friction factors of the vertical joints with the horizontal joints. Fernández [21] performed tests of triplets built with ceramic bricks, subjected to direct shear with a smooth and rough face, representing the horizontal and the vertical joint. The ceramic bricks units with similar characteristics to the specimens collected in the database yielded a quality factor equal to F = 0.5. Cruz [23] performed tests on masonry walls built with concrete blocks with and without the presence of vertical joints to study their effect on strength. Base on Cruz [23] results, Maldonado [24] determined the quality factor for walls built with concrete blocks as F = 0.35.

The ratio of normal stresses acting on the unit $\chi = \frac{f_n}{f_p}$ was determined by Maldonado [24] through a finite element analysis for an isotropic linear-elastic material as a simplified model for masonry. The factor was calibrated for aspect ratios between λ = 0.5 and 2, as

$$\chi = -0.83\lambda + 1.6 \geq 0 \tag{18}$$

3.5. Flexure

For reinforced masonry walls, the equations proposed by Hidalgo [12] and developed by Silva [25] are used. In this case, a parabolic distribution of stresses in the compression zone of the masonry, with an equivalent block of width equal to two thirds of the distance to the neutral axis is generated. For confined masonry walls, there is a contribution of reinforced concrete columns in the flexural strength. An ultimate concrete compressive strain of 0.003 is taken into account and an equivalent strength block as described in ACI 318-19 [26] is used.

3.6. Shear strength estimation

Once all potential failure modes are established, the shear strength of the masonry wall can be determined. Based on the closed-form solution, Fig. 6 shows a flowchart that starts with the estimation of the strain field that begins with the principal strain direction (α, Eq. (8)) and the strain values associated to the first 3 failure modes: (1) masonry in tension, (2) masonry in compression and (3) yielding of reinforcement. Each failure mode has a calibrated expression for either ε_d* or ε_r* (Eqs. (10)–(12)), such that the strain in all materials (masonry and steel) can be determined. Material properties are used to determine stresses in masonry and steel (Fig. 3) for all 3 failure modes, but in this case, aspect ratio (K_c = 0.93) and anisotropy needs to be taken into account by reducing the compressive and tensile stresses of the masonry panel. In the case of anisotropy, the coefficients C_α (Eq. (13)) and $C_{t\alpha}$ (Eq. (15)) are used for compression and tension, respectively. Once stresses are determined, the shear stress in the wall is determined according to Eq. (2) (the largest stress from all 3 failure modes is selected, recalling that either compression failure or reinforcement yielding is considered based on the one that is reached at smaller shear strain). In the case of adherence failure, Eq. (17) provides the estimation of shear

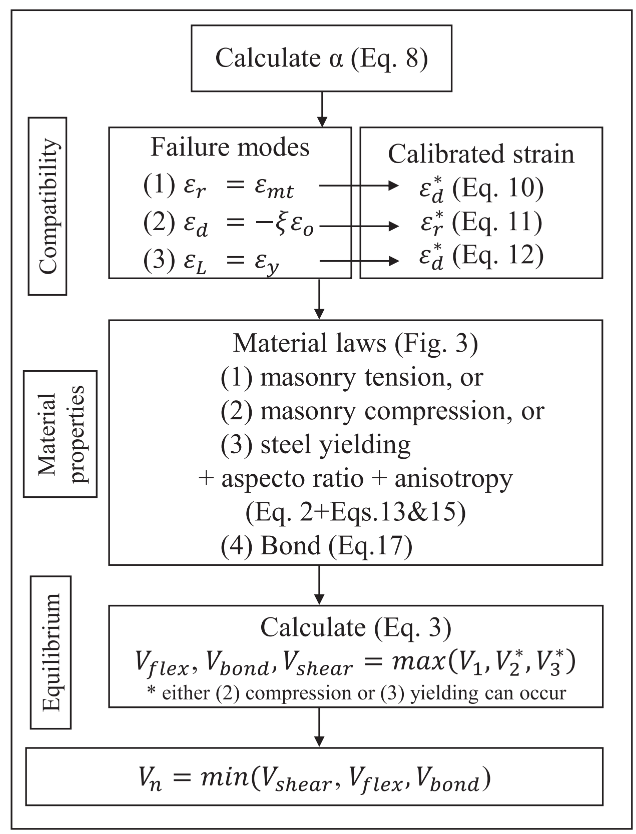

Fig. 6. Flowchart for the proposed closed-form shear model for masonry walls.

Table 1
Reinforced masonry wall characteristics and strength estimations.

Author	Unit type	Specimen	Hw mm	Lw mm	tw mm	Lb mm	tb mm	dw mm	holes %	f'm MPa	ρL %	fyL MPa	ρt %	fyt MPa	ρb %	fyb MPa	N kN	N/f'mAg	Vtest kN	Vflex kN	Proposed model V kN	V/Vt	Failure pred	Reinforced masonry models V [25] kN	V/Vt	V [34] kN	V/Vt
DICTUC [29]	CB	MBH-00-SA01	2050	2030	140	203	140	1624	40	5.0	0.00	0	0.00	0	3.75	474	0	0.00	79	258	98	1.24	Tension	28	0.36	38	0.48
DICTUC [29]	CB	MBH-00-SA02	2050	2030	140	203	140	1624	40	5.0	0.00	0	0.00	0	3.75	474	0	0.00	93	258	98	1.05	Tension	28	0.31	38	0.41
DICTUC [29]	CB	MBH-00-CA01	2050	2030	140	203	140	1624	40	5.0	0.00	0	0.00	0	3.75	474	167	0.12	133	329	138	1.04	Bond	50	0.37	85	0.64
DICTUC [29]	CB	MBH-00-CA02	2050	2030	140	203	140	1624	40	5.0	0.00	0	0.00	0	3.75	474	167	0.12	105	329	138	1.31	Bond	50	0.47	85	0.81
DICTUC [29]	CB	MBH-02-SA01	2050	2030	140	203	140	1624	40	4.7	0.00	0	0.02	593	3.75	474	0	0.00	108	258	96	0.88	Tension	37	0.34	43	0.40
DICTUC [29]	CB	MBH-02-CA01	2050	2030	140	203	140	1624	40	4.7	0.00	0	0.02	593	3.75	474	169	0.13	141	324	135	0.96	Bond	52	0.37	90	0.64
DICTUC [29]	CB	MBH-02-CA02	2050	2030	140	203	140	1624	40	4.7	0.00	0	0.02	593	3.75	474	171	0.13	150	325	135	0.90	Bond	52	0.35	90	0.60
DICTUC [29]	CB	MBH-03-SA01	2050	2030	140	203	140	1624	40	5.3	0.00	0	0.03	593	3.75	474	0	0.00	129	258	104	0.81	Tension	52	0.40	51	0.40
DICTUC [29]	CB	MBH-03-SA02	2050	2030	140	203	140	1624	40	5.3	0.00	0	0.03	593	3.75	474	0	0.00	135	258	104	0.77	Tension	52	0.38	51	0.38
DICTUC [29]	CB	MBH-03-CA01	2050	2030	140	203	140	1624	40	5.3	0.00	0	0.03	593	3.75	474	169	0.11	158	330	140	0.89	Bond	72	0.46	99	0.63
DICTUC [29]	CB	MBH-03-CA02	2050	2030	140	203	140	1624	40	5.3	0.00	0	0.03	593	3.75	474	168	0.11	172	330	140	0.81	Bond	72	0.42	99	0.58
DICTUC [29]	CB	MBH-04-CA01	2050	2030	140	203	140	1624	40	4.7	0.00	0	0.04	593	3.75	474	172	0.13	146	326	135	0.92	Bond	92	0.63	97	0.67
DICTUC [29]	CB	MBH-04-CA02	2050	2030	140	203	140	1624	40	4.7	0.00	0	0.04	593	3.75	474	173	0.13	169	326	134	0.80	Bond	92	0.55	98	0.58
Sierra [27]	CB	MBH-00vd-SA01	2050	3630	140	363	140	2904	40	4.8	0.00	0	0.02	615	0.84	477	0	0.00	133	137	137	1.03	Flexure	113	0.85	80	0.60
Sierra [27]	CB	MBH-00vd-SA02	2050	3630	140	363	140	2904	40	4.8	0.00	0	0.02	615	0.84	477	0	0.00	116	137	137	1.18	Flexure	113	0.98	80	0.69
Sierra [27]	CB	MBH-01vd-SA01	2050	3630	140	363	140	2904	40	4.8	0.02	498	0.02	615	0.84	477	0	0.00	103	137	137	1.33	Flexure	113	1.10	80	0.77
Sierra [27]	CB	MBH-01vd-SA02	2050	3630	140	363	140	2904	40	4.8	0.02	498	0.02	615	0.84	477	0	0.00	138	137	137	0.99	Flexure	113	0.82	80	0.58
Sierra [27]	CB	MBH-02vd-SA01	2050	3630	140	363	140	2904	40	4.8	0.04	498	0.02	615	0.84	477	0	0.00	137	137	137	1.00	Flexure	113	0.83	80	0.58
Sierra [27]	CB	MBH-02vd-SA02	2050	3630	140	363	140	2904	40	4.8	0.04	498	0.02	615	0.84	477	0	0.00	140	137	137	0.98	Flexure	113	0.81	80	0.57
Sierra [27]	CB	MBH-03vd-SA01	2050	3630	140	363	140	2904	40	4.8	0.06	498	0.02	615	0.84	477	0	0.00	145	137	137	0.94	Flexure	113	0.78	80	0.55
Sierra [27]	CB	MBH-03vd-SA02	2050	3630	140	363	140	2904	40	4.8	0.06	498	0.02	615	0.84	477	0	0.00	139	137	137	0.98	Flexure	113	0.82	80	0.57
Sepúlveda [28]	B	MLC-00-CA01	2000	1975	140	198	140	1580	46	9.1	0.00	0	0.00	0	4.25	465	171	0.07	125	331	146	1.18	Tension	122	0.98	123	0.99
Sepúlveda [28]	B	MLC-01-SA01	2000	1975	140	198	140	1580	46	9.1	0.00	0	0.01	599	4.25	465	0	0.00	96	254	128	1.34	Compression	88	0.91	72	0.75
Sepúlveda [28]	B	MLC-02-SA01	2000	1975	140	198	140	1580	46	9.1	0.00	0	0.02	599	4.25	465	0	0.00	112	254	128	1.15	Compression	96	0.86	75	0.67
Sepúlveda [28]	B	MLC-02-SA02	2000	1975	140	198	140	1580	46	9.1	0.00	0	0.02	599	4.25	465	0	0.00	120	254	128	1.08	Compression	96	0.80	75	0.63
Sepúlveda [28]	B	MLC-03-SA01	2000	1975	140	198	140	1580	46	9.1	0.00	0	0.03	599	4.25	465	0	0.00	139	254	128	0.92	Compression	104	0.75	79	0.57
Sepúlveda [28]	B	MLC-03-SA02	2000	1975	140	198	140	1580	46	9.1	0.00	0	0.03	599	4.25	465	0	0.00	125	254	128	1.03	Compression	104	0.84	79	0.63
Sepúlveda [28]	B	MLC-02-CA01	2000	1975	140	198	140	1580	46	9.1	0.00	0	0.02	599	4.25	465	173	0.07	142	332	151	1.06	Tension	139	0.98	131	0.92
Sepúlveda [28]	B	MLC-02-CA02	2000	1975	140	198	140	1580	46	9.1	0.00	0	0.02	599	4.25	465	172	0.07	149	332	151	1.01	Tension	139	0.94	130	0.88
Sepúlveda [28]	B	MLC-02-CA03	2000	1975	140	198	140	1580	46	9.1	0.00	0	0.02	599	4.25	465	165	0.07	130	329	149	1.15	Tension	137	1.05	129	0.99
Sepúlveda [28]	B	MLC-03-CA01	2000	1975	140	198	140	1580	46	9.1	0.00	0	0.03	599	4.25	465	167	0.07	165	330	152	0.92	Tension	146	0.89	133	0.80
Sepúlveda [28]	B	MLC-03-CA02	2000	1975	140	198	140	1580	46	9.1	0.00	0	0.03	599	4.25	465	165	0.07	161	329	151	0.94	Tension	145	0.90	132	0.82
Sepúlveda [28]	B	MLC-04-CA01	2000	1975	140	198	140	1580	46	9.1	0.00	0	0.04	599	4.25	465	166	0.07	152	329	154	1.01	Tension	154	1.01	136	0.89
Sepúlveda [28]	B	MLC-04-CA02	2000	1975	140	198	140	1580	46	9.1	0.00	0	0.04	599	4.25	465	169	0.07	171	331	154	0.90	Tension	155	0.90	137	0.80
Sierra [27]	B	MLC-00vd-SA-01	2000	3620	140	362	140	2896	51	9.2	0.00	0	0.02	616	2.04	477	0	0.00	228	272	208	0.91	Tension	173	0.76	141	0.62
Sierra [27]	B	MLC-00vd-SA-02	2000	3620	140	362	140	2896	51	9.2	0.00	0	0.02	616	2.04	477	0	0.00	241	272	208	0.86	Tension	173	0.72	141	0.59
Sierra [27]	B	MLC-01vd-SA-01	2000	3620	140	362	140	2896	51	9.2	0.03	498	0.02	616	2.04	477	0	0.00	197	272	208	1.05	Tension	173	0.88	141	0.72
Sierra [27]	B	MLC-02vd-SA-01	2000	3620	140	362	140	2896	51	9.2	0.05	498	0.02	616	2.04	477	0	0.00	259	272	208	0.80	Tension	173	0.67	141	0.54
Sierra [27]	B	MLC-02vd-SA-02	2000	3620	140	362	140	2896	51	9.2	0.05	498	0.02	616	2.04	477	0	0.00	208	272	208	1.00	Tension	173	0.83	141	0.68
Sierra [27]	B	MLC-03vd-SA-01	2000	3620	140	362	140	2896	51	9.2	0.08	498	0.02	616	2.04	477	0	0.00	230	272	208	0.90	Tension	173	0.75	141	0.61
Sierra [27]	B	MLC-03vd-SA-02	2000	3620	140	362	140	2896	51	9.2	0.08	498	0.02	616	2.04	477	0	0.00	251	272	208	0.83	Tension	173	0.69	141	0.56
Notes:																					Avg	1.00			0.72		0.65
CB: concrete block		V [25]: Silva																			COV	0.15			0.32		0.23
B: ceramic brick unit		V [34]: Tomazevic																									

stress in the wall. The shear force is later determined (Eq. (3)) for all potential failure modes, including flexure. Thus, the shear strength of masonry walls is determined as the minimum of flexure failure, bond failure and the selected failure between compression, tension and reinforcement yielding.

4. Panel-type model for masonry walls

The database of reinforced masonry walls consists of 41 tests, carried out by Sierra [27], Sepúlveda [28] and by DICTUC S.A. [29], corresponding to 21 specimens made with concrete blocks and 20 with ceramic bricks (Table 1). All specimens had a constant width, equivalent to a block or brick width of 140 mm. They were 2050 mm or 2000 mm tall, for walls built with concrete blocks or ceramic bricks, respectively. The length ranges between 1975 mm and 3630 mm. Thus, the walls presented an aspect ratio H_w/L_w (wall height to length ratio) close to 0.5 or 1.0. The percentage of holes in the units ranged from 40% to 51%. The prismatic strength ranged from 4.8 MPa to 5.3 MPa for walls built with concrete blocks and from 9.1 MPa to 9.2 MPa for walls constructed with ceramic bricks. Eleven masonry walls had longitudinal reinforcement, which do not exceed a ratio of 0.08%. On the other hand, the amount of transverse reinforcement presented a maximum value of 0.04%. The boundary reinforcement ratio varied between 0.8% and 4.3%. About 40% of the specimens included an axial load. In these walls, a constant axial load was applied, which ranged between $0.07f'_mA_g$ and $0.13f'_mA_g$.

The database of confined masonry walls consists of 12 specimens tested by Diez [30], Herrera [31], Muñoz [32] and Ogaz [33], 8 built with ceramic bricks and 4 with concrete blocks (Table 2). The walls had an average width of 140 mm (± 1 mm), similar to the case of reinforced masonry walls. The height varied between 2200 mm and 2400 mm. The length varied between 2400 mm and 3650 mm, yielding also an aspect ratio close to 0.5 or 1. The percentage of holes in the units also varied between 40% and 51%. The prismatic strength varied between 6.0 MPa and 13.5 MPa. The walls do not have longitudinal or transverse reinforcement in the panel, but boundary reinforcement was provided in the columns, whose ratio varied between 1.1% and 1.5%. Only 5 walls had axial load, with values ranging from $0.02f'_mA_g$ and $0.06f'_mA_g$.

All tests were carried out under a cantilever wall condition, fixed at the base, with a variable lateral point load and a constant axial load.

4.1. Predictability of the model

In this section, the performance of the proposed panel model developed for masonry walls is analyzed. This is achieved by comparing the capacity obtained by the model for masonry walls with the experimental capacity observed in the tests (Tables 1 and 2). A summary of the average and coefficient of variation (COV) values of the ratio V_{model}/V_{test} for all walls is shown in Table 3. The average result is 1.0 for reinforced masonry walls with a COV of 0.15, whereas for confined walls, the average is 1.08 with a similar COV (0.14).

In reinforced masonry walls, all failure modes are observed, whereas in confined masonry walls, there are no cases of failure due to bending. The average strength error is less than 10% for all failure modes in both wall types, except in the case of bond failure in confined masonry, with an overestimation of the average strength of 32%. Fig. 7 shows the experimental shear force versus the predicted shear force for reinforced and confined masonry walls. In general, the results fall close to the 45°-angle line that indicates perfect correlation. The model also predicts that 53% of the cases fail in tension, and less than 20% of the cases belong to each of the other failure modes with similar presence number of cases. The failure modes were also estimated from the test reports collected from the literature. However, the authors did not clearly categorize the failure types, such that failure mode was deduced

Table 2
Confined masonry wall characteristics and strength estimations.

Author	Unit type	Specimen	Hw mm	Lw mm	tw mm	Lb mm	tb mm	dw mm	holes %	fm MPa	ρL %	fyL MPa	ρt %	fyt MPa	ρb %	fyb MPa	N kN	N/fmAg	Vtest kN	Vflex kN	Proposed model V kN	Proposed model V/Vt	Proposed model Failure pred	Confined masonry models V [36] kN	V/Vt	V [35] kN	V/Vt
Diez [30]	B	MRG1	2400	2400	139	200	150	1920	41	13.5	0.00	0	0.42	276	1.51	446	0	0.00	162	197	175	1.08	Compression	156	0.97	163	1.01
Diez [30]	B	MRG2	2400	2400	139	200	150	1920	41	13.5	0.00	0	0.42	276	1.51	446	0	0.00	189	197	175	0.93	Compression	156	0.83	163	0.86
Herrera [31]	B	A11	2400	2400	140	200	150	1920	41	12.0	0.00	0	0.42	276	1.51	446	0	0.00	143	196	163	1.14	Tension	118	0.83	165	1.15
Herrera [31]	B	A12	2400	2400	140	200	150	1920	41	12.0	0.00	0	0.42	276	1.51	446	79	0.02	189	237	195	1.03	Tension	136	0.72	165	0.87
Herrera [31]	B	A14	2400	2400	140	200	150	1920	41	12.0	0.00	0	0.42	276	1.51	446	157	0.04	172	278	212	1.24	Tension	154	0.90	165	0.96
Herrera [31]	B	A2	2400	2400	140	200	150	1920	41	12.0	0.00	0	0.42	276	1.51	446	79	0.02	182	237	195	1.07	Tension	136	0.75	165	0.90
Muñoz [32]	CB	C11	2400	2400	140	200	150	1920	40	8.9	0.00	0	0.31	284	1.05	441	137	0.05	177	205	181	1.03	Tension	137	0.77	120	0.68
Muñoz [32]	CB	C12	2400	2400	140	200	150	1920	40	7.0	0.00	0	0.31	284	1.05	441	137	0.06	183	205	169	0.92	Tension	136	0.74	120	0.65
Ogaz [33]	CB	MBH-T1-01	2250	3650	140	200	150	2920	40	6.0	0.00	0	0.27	587	1.05	553	0	0.00	124	282	168	1.35	Bond	113	0.91	146	1.18
Ogaz [33]	CB	MBH-T1-02	2250	3650	140	200	150	2920	40	6.0	0.00	0	0.27	587	1.05	553	0	0.00	130	282	168	1.29	Bond	113	0.87	146	1.12
Ogaz [33]	B	MLC-T1-01	2200	3600	141	200	150	2880	51	6.9	0.00	0	0.27	587	1.05	553	0	0.00	172	284	170	0.99	Tension	126	0.73	207	1.20
Ogaz [33]	B	MLC-T1-02	2200	3600	141	200	150	2880	51	6.9	0.00	0	0.27	587	1.05	553	0	0.00	199	284	170	0.85	Tension	126	0.63	207	1.04
																					Avg	**1.08**			**0.80**		**0.97**
																					COV	**0.14**			**0.12**		**0.19**

Notes:
CB: concrete block; V [36]: Raymondi
B: ceramic brick unit; V [35]: Stafford et. Al

Table 3
Statistical analysis of strength estimate ratio for the proposed model distinguishing different failure modes for reinforced and confined masonry walls.

Failure	Reinforced masonry walls			Confined masonry walls		
	No	Avg.	COV	No	Avg.	COV
All	**41**	**1.00**	**0.15**	**12**	**1.08**	**0.14**
Tension	20	0.96	0.14	8	1.03	0.12
Compression	5	1.10	0.14	2	1.01	0.11
Bond	8	0.95	0.17	2	1.32	0.03
Flexure	8	1.05	0.13			

from the test photos at failure. From about 50% of the specimens, the failure mode can be deduced, with a correct prediction of the failure type for about 80% of them.

4.2. Analysis of general trends of the model

In this section, the general trends of the model with respect to relevant parameters of masonry walls are shown. The input parameters of the model are chosen, which correspond to the characteristics that define the wall properties, such as the aspect ratio (H_w/L_w), the prismatic resistance of the element, the axial compression stress ($N/(f'_m A_g)$) and the transverse, longitudinal and boundary steel quantities, as well as the principal direction angle. The dependence of the model to the variations of each parameter is evaluated, considering that the lower the dependency the better its physical behavior is incorporated in the analysis. This is shown graphically by the ratio between the predicted shear strength of the model and the experimental shear with respect to the variation of the studied parameters. Trend lines are also shown for all cases. The trend lines are the best-fit linear curves of the data, which shows how the strength ratio (for the proposed model) changes with a specific parameter (e.g., axial load, aspect ratio). Therefore, if a trend line shows a constant value (no slope) equal to one that means that the strength is well captured independent of the value of the specific parameter. Having moderate slopes in the trend lines indicate that the dependency of the strength model to the specific parameter is correctly incorporated.

Fig. 8 shows the strength ratio versus selected parameters. The data is separated between reinforced masonry walls (blue) and confined masonry (red) walls, together with the trend lines (consistent colors). The trend lines are shown for cases where the range of parameters covers at least about 50% of the total range for the walls. The overall trend lines for all walls is also included (black). Regarding the aspect ratio (Fig. 8a), the data concentrates the values close to aspect ratios of 1 or 0.5, where the strength ratio for all specimens almost does not present dependency to the aspect ratio (trend line), indicating that the strength model correctly captures such parameter. Similar situation is observed for other parameters (Fig. 8) such as: prismatic compressive strength (f'_m), principal strain/stress direction (α), axial stress level ($N/(f'_m A_g)$), transverse yield force per area ($\rho_t f_{yt}$), longitudinal yield force per area ($0.3\rho_b f_{yb} + \rho_l f_{yl}$). In these cases, there is a low dependency to the different parameters, where for the entire range of each parameters, the trend line of the strength ratio for all specimens varies less than 10% in all cases. When the specimens are separated between reinforced and confined masonry walls, the dependency is still small, with similar values as for the entire database, which confirms that the model captures correctly the response for both types of walls.

5. Comparison with other models

In this section, other formulations available in the literature are presented in order to compare their performance against the proposed model (Tables 1 and 2). All comparison formulations presented here are related to design of masonry walls. They provide shear strength equations with code design applications. However, all of them propose expressions with either a safety factor or a strength reduction factor, which is set as one for the current analysis. Such that the expressions are not as conservative as it would be for design. The comparison, however, is intended to show the capability of other approaches to provide good predictions of masonry wall strength, and as shown with the different formulations and different terms, a unique expression cannot easily predict the strength for all specimens (e.g., separated between reinforced and confined masonry walls). The unique expression proposed in this research can deal with different configurations including all relevant parameters.

5.1. Reinforced masonry walls

5.1.1. Model by Silva [25]

Silva [25], for walls with partially grouted holes and low horizontal reinforcement ratios (≤0.06%), recommends calculating the nominal shear strength (V_n) as,

$$V_n = V_m + V_s \tag{19}$$

$$V_m = 0.4\tau_o A_g + 0.25N \leq 0.7\tau_o A_g \tag{20}$$

$$V_s = 0.5\rho_t f_{yt} t_w min(L_w, H_w) \leq V_m \tag{21}$$

where V_m and V_s are the masonry panel and reinforcement contribution, respectively, τ_o is the basic shear stress, N the axial load, and t_w is the masonry panel thickness.

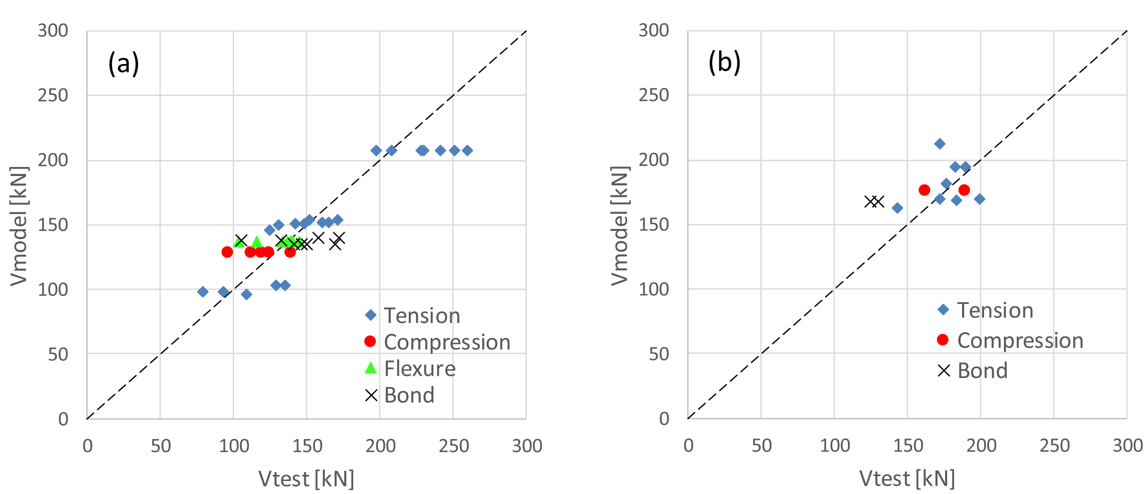

Fig. 7. Strength ratio V_{model}/V_{test} for different failure modes – (a) reinforced masonry walls, and (b) confined masonry walls.

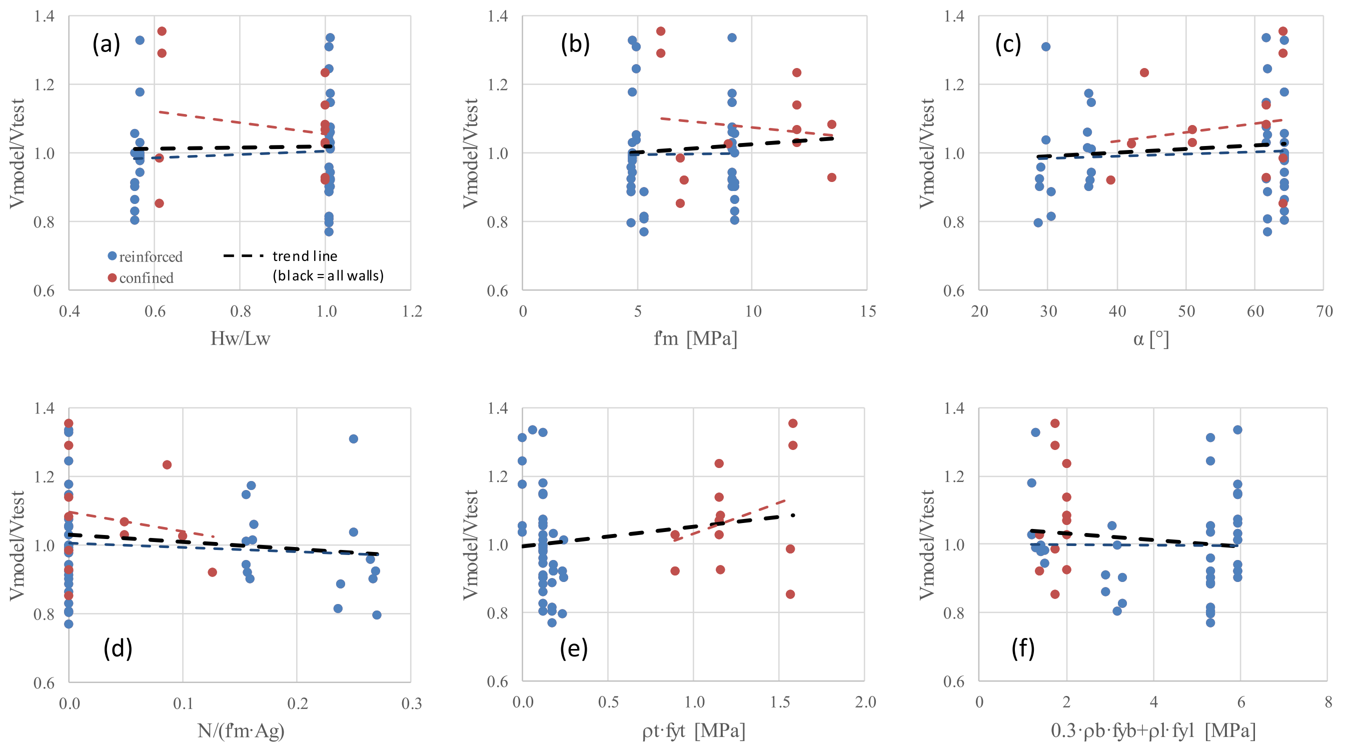

Fig. 8. Sensitivity analysis for masonry walls – (a) aspect ratio, (b) prismatic strength, (c) principal stress/strain angle, (d) axial load level, (e) transverse reinforcement force per unit area, and (f) longitudinal reinforcement force per unit area.

5.1.2. Model by Tomazevic [34]

Tomazevic [34] proposes a masonry shear strength model that incorporates the contribution of the masonry panel and reinforcement, as

$$H_{sd,r} = H_{sd,w} + C_{rh} \cdot H_{sd,rh} + H_{dd,rv} \tag{22}$$

$$H_{sd,w} = A_g \frac{f'_{mt}}{b} \sqrt{\frac{f_n}{f'_{mt}} + 1} \tag{23}$$

$$H_{sd,rh} = 0.9d \frac{A_t f_{yt}}{s} \tag{24}$$

$$H_{dd,rv} = 0.806 \cdot n \cdot d_{bl}^2 \sqrt{f'_m f_{yl}} \leq 0.25 d_{bl}^2 f_{yl} \tag{25}$$

where $H_{sd,w}$ is the masonry contribution to shear strength, $H_{sd,rh}$ is the horizontal web reinforcement contribution to shear strength, $H_{dd,rv}$ is the vertical web reinforcement contribution to shear strength, C_{rh} is a reduction factor of the transverse reinforcement, set as 0.3, f'_{tm} is the tensile masonry panel strength, b is a shear distribution factor (1.1 for wall with aspect ratio less or equal to 1 and 1.5 for aspect ratio of 1.5), f_n is the wall axial stress (N/A_g), d is the effective wall depth, A_t is the total transverse steel area, s is the transverse steel spacing, n is the number of longitudinal bars, and d_{bl} is the longitudinal bar diameter.

5.2. Confined masonry walls

5.2.1. Model by Stafford Smith and Riddington [35]

The work by Stafford Smith and Riddington [35] proposes a set of three independent equations for shear strength of masonry walls divided into the potential failure modes: bond, tension and compression by modeling the masonry panel as a strut, as

$$V_s = \frac{\tau_o L_m t_w}{\left[1.43 - \mu\left(0.8\frac{h_m}{L_m} - 0.2\right)\right]} \tag{26}$$

$$V_t = 1.72 A_g f'_{tm} \tag{27}$$

$$V_c = 4 f'_m cos^2(\theta) \sqrt[4]{I_c h_m t_w^3} \tag{28}$$

where L_m is the wall panel length, μ is the coefficient of friction between the mortar and the unit, h_m is the wall panel height, θ is the complement of α ($\theta = \pi/2 - \alpha$), and I_c is the column inertia.

5.2.2. Model by Raymondi [36]

The Chilean code, NCh 2123 (2003) [37], uses an admissible force that corresponds to about 50% of the actual strength (safety factor of 2), based on the expression by Raymondi [36]. The strength expression by Raymondi [36] is,

$$V_n = (0.45\tau_o + 0.24 f_n) A_g \tag{29}$$

5.3. Comparison

A summary of the results obtained for each type of wall and a comparison of the proposed panel type model with the models from the literature is shown in Fig. 9 and Table 4. The models by Silva [25] and Tomazevic [34] underestimate the capacity of the walls by about 30% and present a high COV, given that they are very sensitive to the area of the wall panel and the contribution of the transverse reinforcement. In the case of the model of Stafford Smith and Riddington [35], although the axial load and the reinforcement are not taking into account in the model, the strength is well predicted, but with larger COV than the proposed model. The equation by Raymondi [36] also does not take into account the effect of the reinforcement, but considers the axial load. However, the model shows an underestimation of average strength of 20% with an adequate COV. In all cases, the proposed model presents a better combination of strength prediction and low COV.

6. Conclusions

In this work, a panel model is proposed for masonry walls either reinforced or confined based on a model originally developed for short walls and other reinforced concrete elements, providing a novel

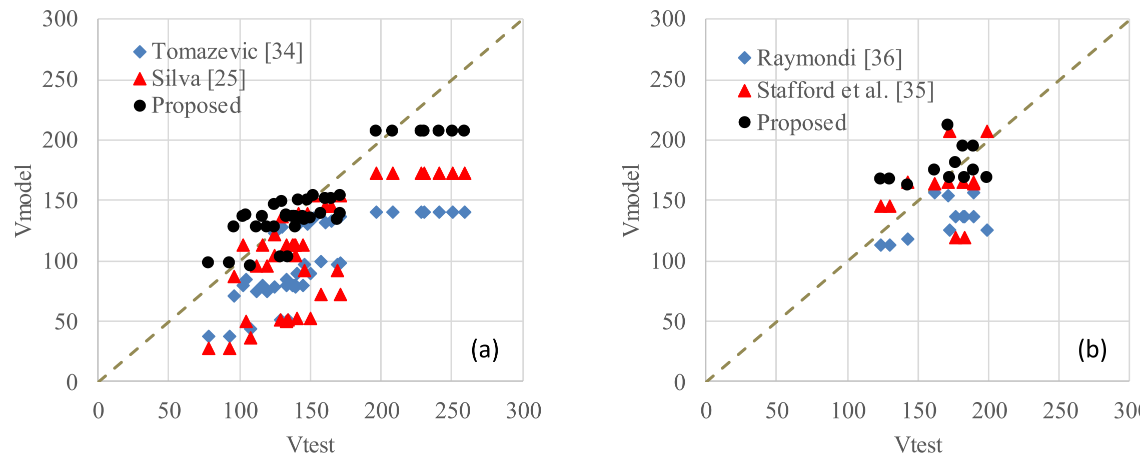

Fig. 9. Strength ratio V_{model}/V_{test} including models from literature – (a) reinforced masonry walls, and (b) confined masonry walls.

Table 4
Statistical analysis of strength estimate ratio of models from the literature for reinforced and confined masonry walls.

Reinforced masonry walls			Confined masonry walls		
Model	Avg.	COV	Model	Avg.	COV
Silva [25]	0.72	0.32	Stafford et al. [35]	0.97	0.19
Tomazevic [34]	0.65	0.23	Raymondi [36]	0.8	0.12
Proposed	1.00	0.15	Proposed	1.08	0.14

formulation that can be applicable to both materials. The modifications required for adaptation to masonry walls include its anisotropy and bond failure (based on a Mohr-Coulomb model) not present in reinforced concrete elements. The effect of the degradation of the compressive and tensile strength due to the inclination between the applied axial load and the vertical mortar joint is also analyzed.

The accuracy of the model is revised comparing the shear strength predictions of the model with a database of 53 specimens comprising reinforced (41) and confined (12) masonry walls. The ratio between the predicted shear and the experimental shear strength gives an average and a coefficient of variation (COV) of 1.0 and 0.15, respectively for reinforced walls, and 1.08 and 0.14 for confined walls, which indicates that the model satisfactorily predicts the shear capacity of masonry walls. The failure mode that predominates is tension (53% of the cases) with correct estimation of the capacity on average. In most cases, the strength ratio presents an average error less than 10% for both types of walls, except for the case of bond failure in the case of confined walls where the average error increases to 32%.

In order to study the dependency of the predictions to common model parameters, the shear strength ratio between the model and the experiments is compared with selected parameters. All selected parameters (aspect ratio, longitudinal reinforcement force per area, transverse reinforcement for per area, axial load level, compressive strength of masonry, and principal strain/stress direction) show little dependency for the strength ratio, which indicates a good incorporation of the parameter in the physical behavior of the shear strength mechanism. In general, the strength ratio varied less than 10% for the overall range of parameters.

The proposed model is also compared with models from the literature. Considering that several models from the literature are intended for shear design, the comparison is intended to show the capability of the current approach to capture the capacity for different types of walls, which is commonly not possible for formulations from the literature. For reinforced masonry walls, the models from the literature underestimate the capacity of the walls, while the proposed model yields an average of 1.0. For confined walls, there is also an underestimation of the capacity, but to a lesser extent. In general, the proposed model presents a better combination of strength prediction and low COV, being capable of capturing the strength for all types of walls and for all failure modes.

Appendix A. Supplementary material

Supplementary data to this article can be found online at https://doi.org/10.1016/j.engstruct.2019.109900.

References

[1] Kassem W, Elsheikh A. Estimation of shear strength of structural shear walls. J Struct Eng 2010;136(10):1215–24.
[2] Vecchio FJ, Collins MP. The modified compressional-field theory for reinforced concrete elements subjected to shear. J Am Concrete Inst 1986;83(22):219–31.
[3] Massone LM, Álvarez JE. Shear strength model for reinforced concrete corbels based on panel response. Earthquakes Struct 2016;11(4):723–40.
[4] Massone LM, Orrego GN. Analytical model for shear strength estimation of reinforced concrete beam-column joints. Eng Struct 2018;173:681–92.
[5] Massone LM, Ulloa MA. Shear response estimate for squat reinforced concrete walls via a single panel model. Earthquakes Struct 2014;7(5):647–65.
[6] Massone LM. Strength prediction of squat structural walls via calibration of a shear - flexure interaction model. Eng Struct 2010;32(4):922–32.
[7] Massone LM, Melo F. General closed-form solution for shear strength estimate of RC elements based on panel response. Eng Struct 2018;172:239–52.
[8] Wang G, Dai JG, Teng JG. Shear strength model for RC beam - column joints under seismic loading. Eng Struct 2012;40:350–60.
[9] Page A, Marshall R. The influence of brick and brickwork prism aspect ratio on the evaluation of compressive strength. Proceedings of the 7th international brick masonry conference. 1986. p. 653–64.
[10] Hamid A, Drysdale R. Concrete masonry under combined shear and compression along the mortar joints. ACI J 1980;77(5):314–20.
[11] Naraine K, Sinha S. Stress-strain curves for brick masonry in biaxial compression. J Struct Eng 1992;118(6):1451–61.
[12] Hidalgo P. Development of design provisions for reinforced masonry buildings in Chile (in Spanish). Anales de la Universidad de Chile 1989;5(21):431–73.
[13] Yu HW, Hwang SJ. Evaluation of softened truss model for strength prediction of reinforced concrete squat walls. J Eng Mech-ASCE 2005;131(8):839–46.
[14] Tomazevic M, Bosiljkov V, Lutman M. Robustness of hollow clay masonry units and seismic behaviour of masonry walls. Constr Build Mater 2006;20:1028–39.
[15] Drysdale R, Hamid A. Anisotropic Tensile Strength Characteristics of Brick Masonry. Proc,Sixth Int Brick Masonry 1982:143–53.
[16] Dhanasekar M, Haider W. Explicit finite element analysis of lightly reinforced masonry shear walls. Comput Struct 2008;86(1–2):15–26.
[17] Dialer C. Some remarks on the strength and deformation behavior of shear stressed masonry panels under static monotonic loading. In: Proceedings of the 9th international Brick/Block masonry conference; 1991, vol. 1. p. 276–83.
[18] Charry J. Experimental study of the behavior of brick walls under lateral loads (in Spanish). Doctoral Thesis in Civil Engineering. Politecnic University of Catalunya; 2010.
[19] Crisafulli F. Seismic behaviour of reinforced concrete structures with masonry infills. Doctoral Thesis in Civil Engineering. University of Canterbury; 1997.
[20] Cabezas F. Analytical estimation of the shear strength of confined masonry walls by the Crisafulli model (in Spanish). Civil Engineering thesis. University of Chile; 2011.
[21] Fernández G. Experimental study of the shear strength of masonry of ceramic units (in Spanish). Civil Engineering thesis. University of Chile; 1986.
[22] Delfín F, Bullemore M. Experimental study of the adhesion between mortar and

concrete blocks (in Spanish). Civil Engineering thesis. University of Chile; 1968.
[23] Cruz J. Study of the brick walls (in French). Doctoral Thesis in Civil Engineering. Universite de. Marne la Vallee 2002.
[24] Maldonado C. Analytical estimation of the shear strength of confined masonry walls by a strut-and-tie model. Modified Crisafulli model (in Spanish). Civil Engineering thesis. University of Chile; 2013.
[25] Silva D. Recommendations for the design of reinforced masonry walls by the strength method (in Spanish). Civil Engineering thesis. University of Chile; 2005.
[26] ACI Committee 318. Building Code Requirements for Reinforced Concrete (ACI 318-19) and Commentary (ACI 318 R-19). American Concrete Institute; 2019. Detroit, Mich.
[27] Sierra G. Experimental study of the influence of vertical reinforcement on reinforced masonry walls subjected to cyclic lateral load (in Spanish). Civil Engineering thesis. University of Chile; 2002.
[28] Sepúlveda M. Influence of horizontal reinforcement on the seismic behavior of masonry walls (in Spanish). Civil Engineering thesis. Pontifical Catholic University of Chile; 2003.
[29] DICTUC SA. Cyclic shear tests of masonry walls of concrete blocks. Reports 1 to 4 for the Instituto Chileno del Cemento y del Hormigón, Chile; 2002.
[30] Diez J. Experimental study of masonry walls subjected to lateral loading (in Spanish). Civil Engineering thesis. University of Chile; 1987.
[31] Herrera E. Effect of vertical load on the behavior of reinforced masonry walls subjected to cyclic lateral load (in Spanish). Civil Engineering thesis. University of Chile; 1992.
[32] Muñoz W. Experimental study of the behavior of masonry walls of concrete blocks subjected to cyclic lateral load (in Spanish). Civil Engineering thesis. University of Chile; 1992.
[33] Ogaz O. Experimental study of masonry walls with openings and reduced amount of reinforcement subject to cyclic lateral load (in Spanish). Civil Engineering thesis. University of Chile; 2004.
[34] Tomazevic M. Earthquake-Resistant Design of Masonry Buildings. Imperial College Press; 1999. p. 109–62.
[35] Stafford Smith B, Riddington JR. The design of masonry infilled steel frames for bracing structures. Struct Eng 1978;56B(1):1–7.
[36] Raymondi V. Proposed draft design and calculation of reinforced masonry with columns and beams (in Spanish). Civil Engineering thesis. University of Chile; 1990.
[37] NCh 2123. Of 97. Mod 2003. Confined masonry - Design and calculation requirements (in Spanish). Instituto Nacional de Normalización – INN Chile; 2003. p. 11–14.